A Centre-triggered Magnesium Fuelled Cathodic Arc Thruster Uses Sublimation to Deliver a Record High Specific Impulse

Supplementary Material

Methods – Ballistic Pendulum

A ballistic pendulum was used to measure momentum rather than an electronic load cell. The rapidly changing electromagnetic fields present in the plasma discharge would induce currents in electronic components, creating noise that could mask the signal of a load cell [34]. Instead, momentum transfer can be determined by measuring the velocity and mass of a ballistic pendulum struck by the plasma and illustrated in figure S1.

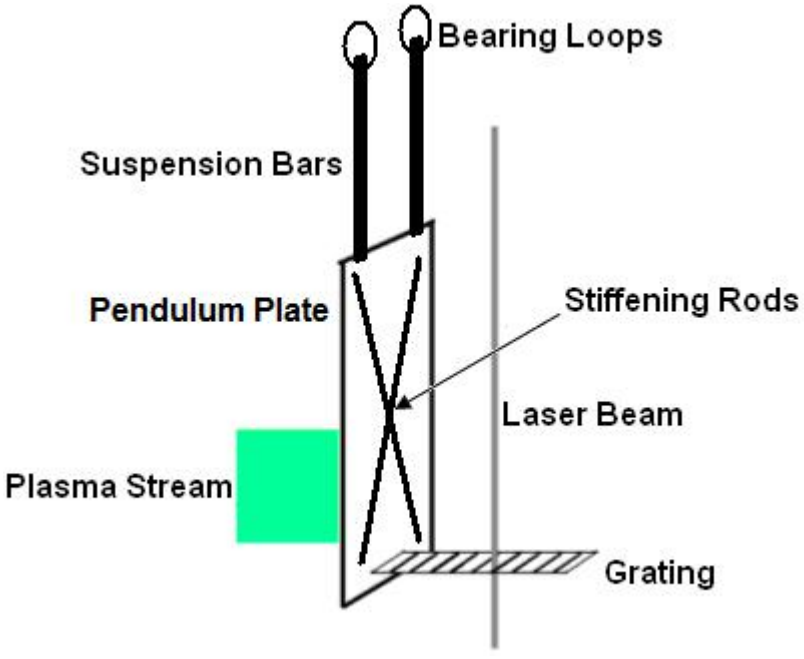

Figure S 1: Ballistic pendulum used to measure plasma impulse.

The pendulum mass was determined by weighing before and after the data run, while the velocity was measured using a laser beam being blocked by a periodic

opacity grid attached to the pendulum. This grid was a series of lines of black ink, printed onto a small plate of thin overhead transparency film at regular intervals of 1.7mm. Laser light was shone onto the grid with the transmitted light being imaged onto a photodiode by mirrors; the photodiode signal was captured by a Digital Storage Oscilloscope (DSO). Variations in light intensity caused by the lines on the grid occluding the laser beam as the pendulum swings create repeating features in the photodiode signal, while the known separation in space of the gridlines allows the determination of the displacement of the pendulum. Examining the DSO trace allowed the determination of the period between two intensity peaks, or troughs, giving the amount of time it took the pendulum to move a given distance. An example photodiode trace is shown in figure S2, together with typical arc current and voltage traces.

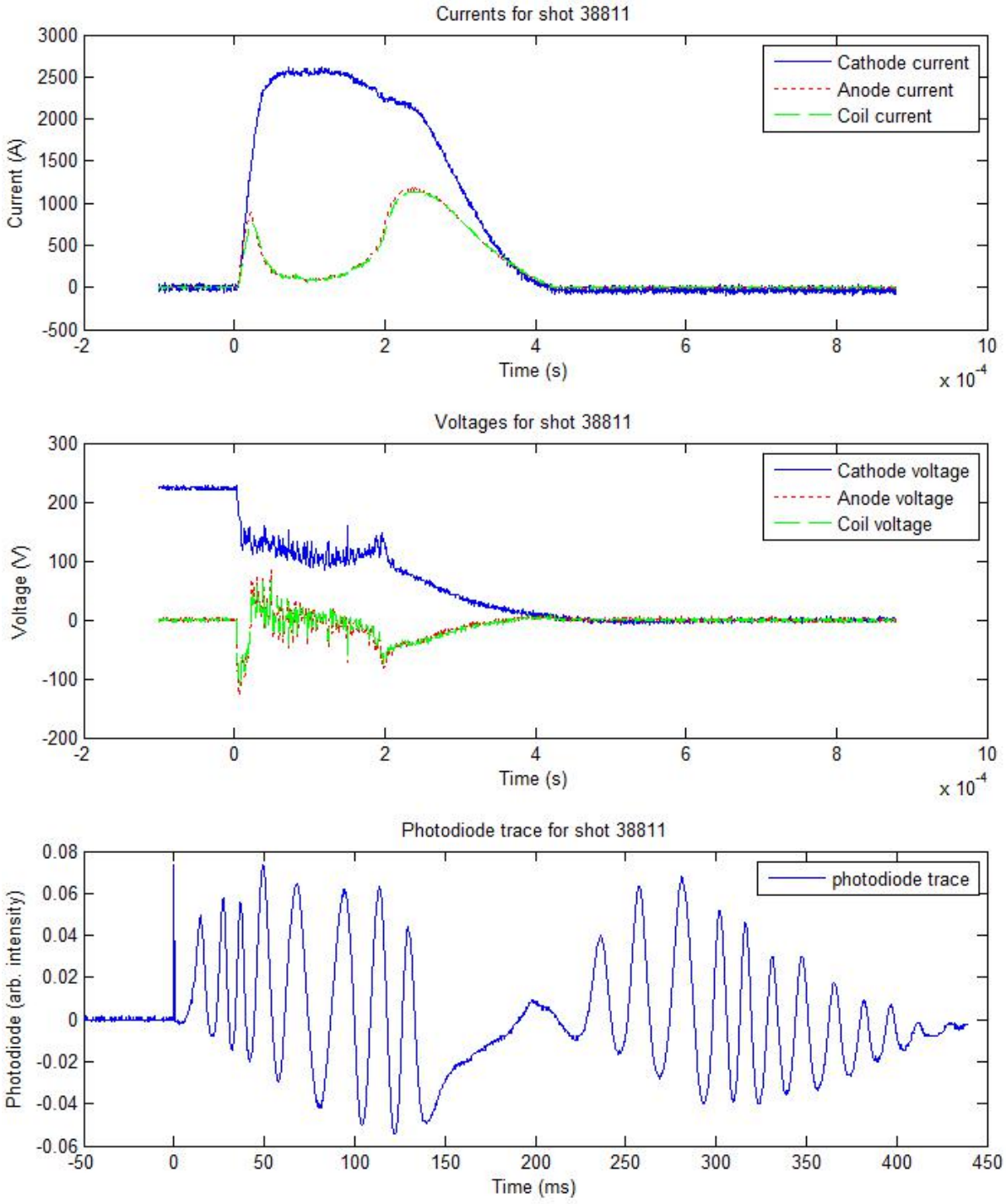

Figure S 2: Typical traces of currents, voltages and photodiode, with coil installed in chamber.

Knowing the feature pitch and the time between features, the velocity of the pendulum can be deduced. Measuring the mass of the pendulum (generally between 4.6 and 4.8g) allows its momentum to be calculated, and the average net force experienced by the pendulum is determined by dividing the impulse by the duration of the pulse. So long as the pendulum is correctly placed, so that it can

swing back along the line of plasma travel, it can give a precise measurement of plasma momentum, though the accuracy of that measurement is limited by a number of factors discussed below.

Firstly, not all of the ions will adhere to the surface of the pendulum; some will stick while others will bounce off. Since these experiments required the oxide layer to be cleaned off the cathode surface, the ions in all pulses examined in this research would be incident on thin layers of deposited cathode material. Literature values of the proportion of metal ions adhering onto a surface of the same species (sticking coefficient) tend to be close to unity; van Velduizen and de Hoog show a sticking coefficient of 0.8 for copper ions, on copper for example [25]. If we assume that 80% of all the ions stick to the metal film on the surface of the pendulum, then the remaining 20% would rebound with a random velocity and angle, imparting some degree of extra momentum to the pendulum. Taking into account the random nature of the resultant trajectories, to be conservative we assumed that the 20% of rebounding ions all collide elastically and have the same average velocity as the 80% that stick. This means that while 80% of the ions stick to the surface, transferring all of their momentum, 20% will rebound from the surface at the same speed but in the opposite direction, transferring twice their original momentum to the pendulum. The pendulum momentum will thus be 1.2 times the momentum carried by the plasma, so multiplying by a factor of 5/6 will account for this effect.

Secondly, some of the impacting ions will sputter atoms from the surface of the metal film, thus creating momentum artefacts as these sputtered atoms depart from the pendulum. This is not thought to be a major effect in our measurements for a number of reasons, chief among them being the low sputter yield of ions at the energies measured in pulsed arc plasmas. The self-sputter rates of ions at the energies in question are less than 8%, and in most cases is closer to 2% [28, 29]. Also, the energy carried by these sputtered atoms is generally quite low; only a few eV compared to the 100-200eV of an impacting ion, which means that the momentum artefact generated by a given sputtered atom will be small [27-29]. Additionally, these atoms are released in a wide range of directions, rather than a directed beam, which would tend to cause the momentum components parallel to the film surface to

cancel [35]. Taking these together shows that the sputtering artefact would be less than 1% hence we have broadened the uncertainty bounds of our thrust measurements by an additional 1% to ensure that we account for this.

Quantifying Uncertainties

The data for fuel specific impulse were derived from measured thrusts, integrated cathode currents and cathode erosion rates. Care was taken when installing the pendulum to ensure that geometric factors affecting pendulum response were minimised, with the resultant thrust uncertainty being 3%, derived as follows.

Construction, Handling and Placement Errors

The pendulum was constructed by hand. While care was taken during manufacture and handling, tolerances will lead to the following potential errors: 1) pendulum geometry, 2) grid geometry, and 3) the contribution of a structure to stop the swinging of the pendulum that acted as a momentum brake.

The pendulum plate must intersect all the plasma and be perpendicular to the plasma flow. If not, then the plasma momentum will not be fully transferred as linear momentum to the pendulum. This would result in a misrepresentation of the total plasma momentum. Also, if the plasma impact site is located far from the support wires, the entire pendulum can twist. These effects were minimised by locating the pendulum close (~10mm) to the mouth of the anode so that the pendulum plate will intersect all the plasma flow, and so that the orientation of the plate with respect to the plasma flow can be measured. For the case where the pendulum is located further from the anode mouth, due to the coil, adjustments were made to account for the incomplete capture of the plasma plume. Twisting was minimised by using two support wires separated by a distance greater than the diameter of the plasma flux tube. By taking care to place the pendulum close to the anode mouth and perpendicular to the plasma flow to within 5 degrees, and measuring this with rule and protractor, the estimated uncertainty is 0.5% from positional sources.

The laser detection grid must be placed so that it is parallel to the direction of plasma travel and perpendicular to the laser beam. Thus the small angle approximation can be used, treating the grid as approximately level for short distances away from the "at-rest" vertical position, allowing the features on the photodiode trace to be interpreted as representing features at a fixed distance. If the grid is bent or twisted in any fashion, then the apparent feature separation would be larger than the true separation by a factor of $sec(t)cos(d)$, where t is the angle of horizontal twist and d is the angle of grid plane dip. Twist angles result in greater apparent distance between features, while angles of dip (or rise) result in lower apparent distances between features. Typical construction and installation of the grid resulted in angles of dip and twist measured to be less than 10 degrees. Visual inspection with the aid of a protractor was carried out during construction of each pendulum, and revealed errors of no more than 5 degrees. Visual inspection of the pendulum before and after each thrust measurement run revealed no greater deviation than 5 degrees from horizontal for the grid. Thus the total deviation for the grid would be less than 10 degrees from horizontal, with twist angles being kept to below 5 degrees. The maximum error from these sources was estimated to be 1.1%.

The momentum brake had to be added to the system in order to force the system to slow between shots. Otherwise, the pendulum was observed to keep swinging for minutes after a pulse was fired at it. The brake was placed so that it pushed on the pendulum at the pendulum's rest position, disturbing it from rest by less than 5mm. The angle induced by this motion was taken into account when considering position errors, as discussed in the preceding paragraph.

Approximations due to Modelling Assumptions

It is assumed that during its initial motion the pendulum is moving linearly, and so the moment of inertia of the system can be neglected. This is a defensible assumption in that horizontal movement of a few millimetres for a pendulous body with the measurement grid approximately 210mm from the fulcrum results in angles of swing of only a few degrees. Typical placement of the laser beam on the grid

would result in measurement being cut off after 20-25mm of pendulum swing, as the pendulum plate would swing into the beam path and scatter the beam. Thus the maximum angle of swing was less than 8 degrees, making the uncertainty in using a small angle approximation less than 0.25%.

The sum of the various thrust measurement uncertainties is 1.85%. These uncertainties are random uncertainties, and would contribute to the sampling error as evaluated by the Standard Error of the Mean (SEM). There is agreement between the uncertainties estimated in this section and the SEMs found from experimental data, which were below 2% in almost all data sets. In order to remain conservative, we round this uncertainty up to 2% and add an additional 1% to the thrust uncertainty to account for sputtering, thus the total uncertainty for each thrust measurement is 3%.

Statistical analysis of integrated cathode currents indicate a standard error of the mean of less than 2%; again, 2% uncertainty in integrated cathode current was selected to be conservative. Certain of the cathode erosion trends were highly subject to noise, so an erosion uncertainty of 10% was chosen. Totalling these contributions, we arrive at an uncertainty value of 15% for specific impulse.

The JPE measurement uncertainty was 20%, with contributions from uncertainties in the erosion rate (10%), measurement of thrust (6%, as it depends on the square of thrust) and integrated cathode current (2%). A further 2% was added to account for the uncertainty of the measured energy expenditure due to the uncertainties of current and voltage measurements in the external circuit. To verify this, statistical analyses were performed on the measured energy expended results and a standard error of less than 2% was found, thus this uncertainty was assigned to energy expended.

Chamber Geometry and Focussing Adjustments

The chamber used for these experiments was a semi-toroid, with the cathode/anode assembly paced as per figure S3 [36]. The addition of the coil forced the change in pendulum location, which necessitated calibration with the prior thrust

measurements due to the greater distance between the cathode and the pendulum, and the reduction in the solid angle subtended by the pendulum. The pendulum was reversed, so that the grid was now upstream of the plate (opposite to fig. S1), in order to allow the laser access to the grid via a viewport.

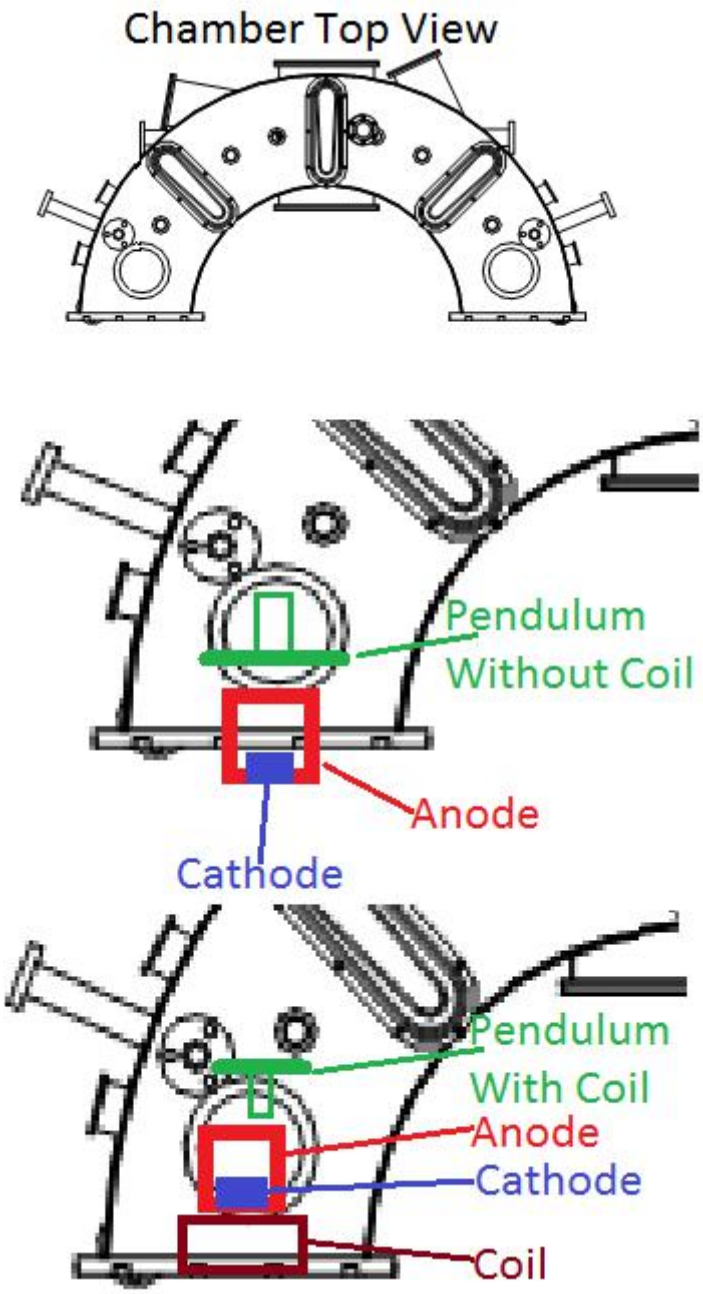

Figure S 3: Chamber geometry, including cathode, anode, coil and pendulum locations.

The pendulum was located further from the cathode and displaced horizontally, rather than immediately in front of the anode mouth. Results from experiments performed with the coil windings insulated from the plasma and earthed

(thus generating no magnetic field) were compared to those undertaken at the same conditions without the coil in place to adjust the results. These plots are shown in figure S4.

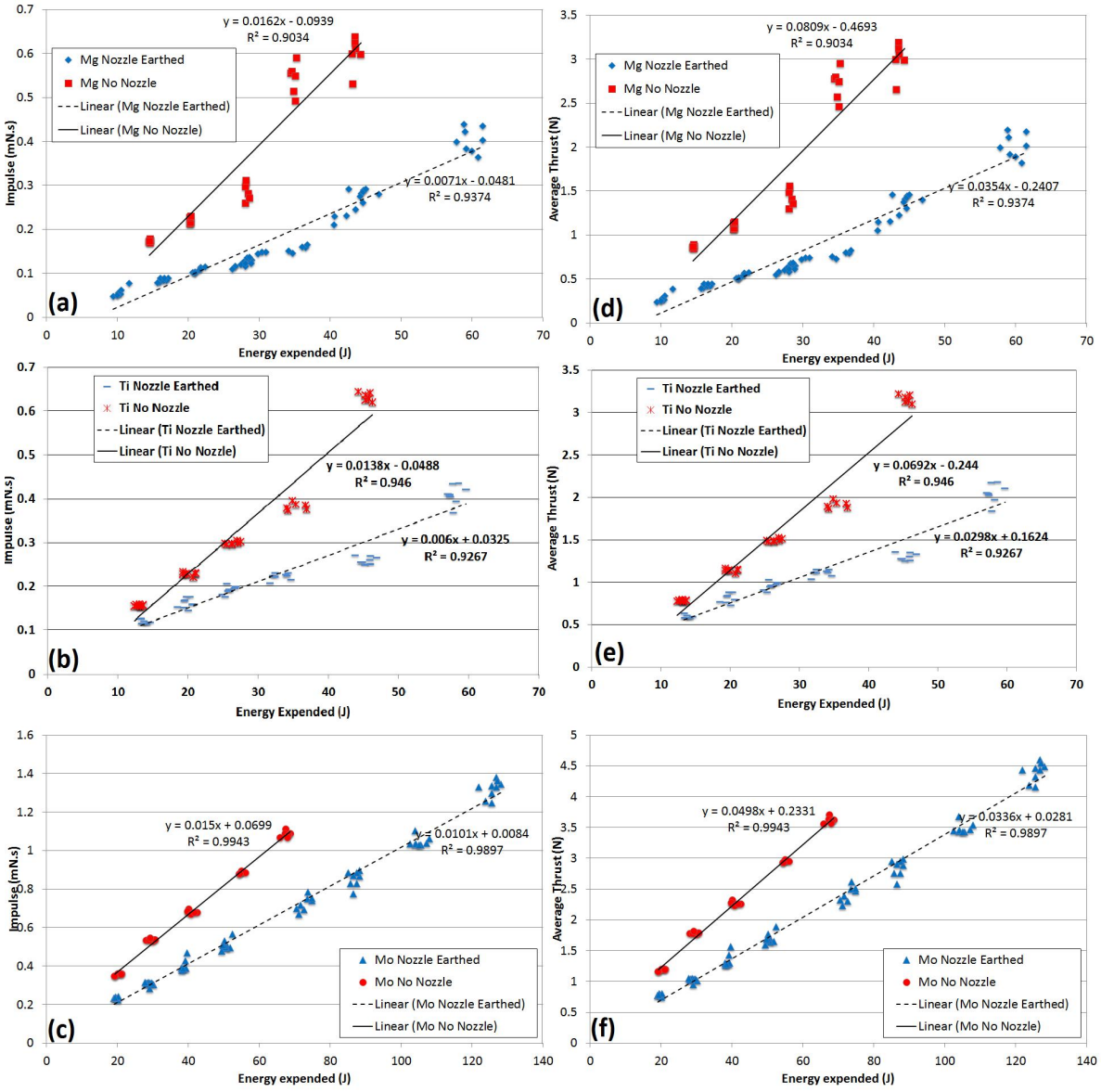

Figure S 4: Plots of impulse and thrust as a function of energy expended for three materials tested with and without magnetic nozzle enhancement; Mg and Ti pulses are 200µs long while Mo pulses were 300µs. Linear fits to the data are shown with equations and R^2 coefficients.

The magnetic nozzle-assisted thrust measurements were adjusted by multiplying the measured thrust data by the ratio between the two trendline slopes in the above graphs to compensate for the change in geometry. All results from experiments performed with the coil in place were multiplied by the Mo ratio. The Mo ratio was chosen because the Mo plots had the highest correlation coefficients

and because the Mo ratio was the smallest derived, thus leading to a more conservative measure of impulse.

After geometric adjustment was performed a deposition study was undertaken to determine the angular spread of the plasma plume with and without the coil present at the location of the pendulum. Titanium plasma was used to study this, with 1100 arcs at 200μs duration and 200V_{ch} struck so that the exhaust plume was deposited onto a sheet of overhead transparency film, with the sheet being attached to the pendulum at the correct mounting location in the chamber. The deposition patterns were measured by optical scanning and processed using ImageJ to determine the half-width to half maximum for each of the optical density profiles, and then approximating each plume as a Gaussian curve. A calibration factor of 0.915 was obtained by comparing the standard deviations of the optical density curves to the area of the pendulum, as the magnetic field focussed the plasma. This meant that the geometrically-adjusted values had to be reduced slightly, so as not to over-compensate for the observed trends. The deposition patterns are included as figure S5 with horizontal transects of the optical density profiles inset.

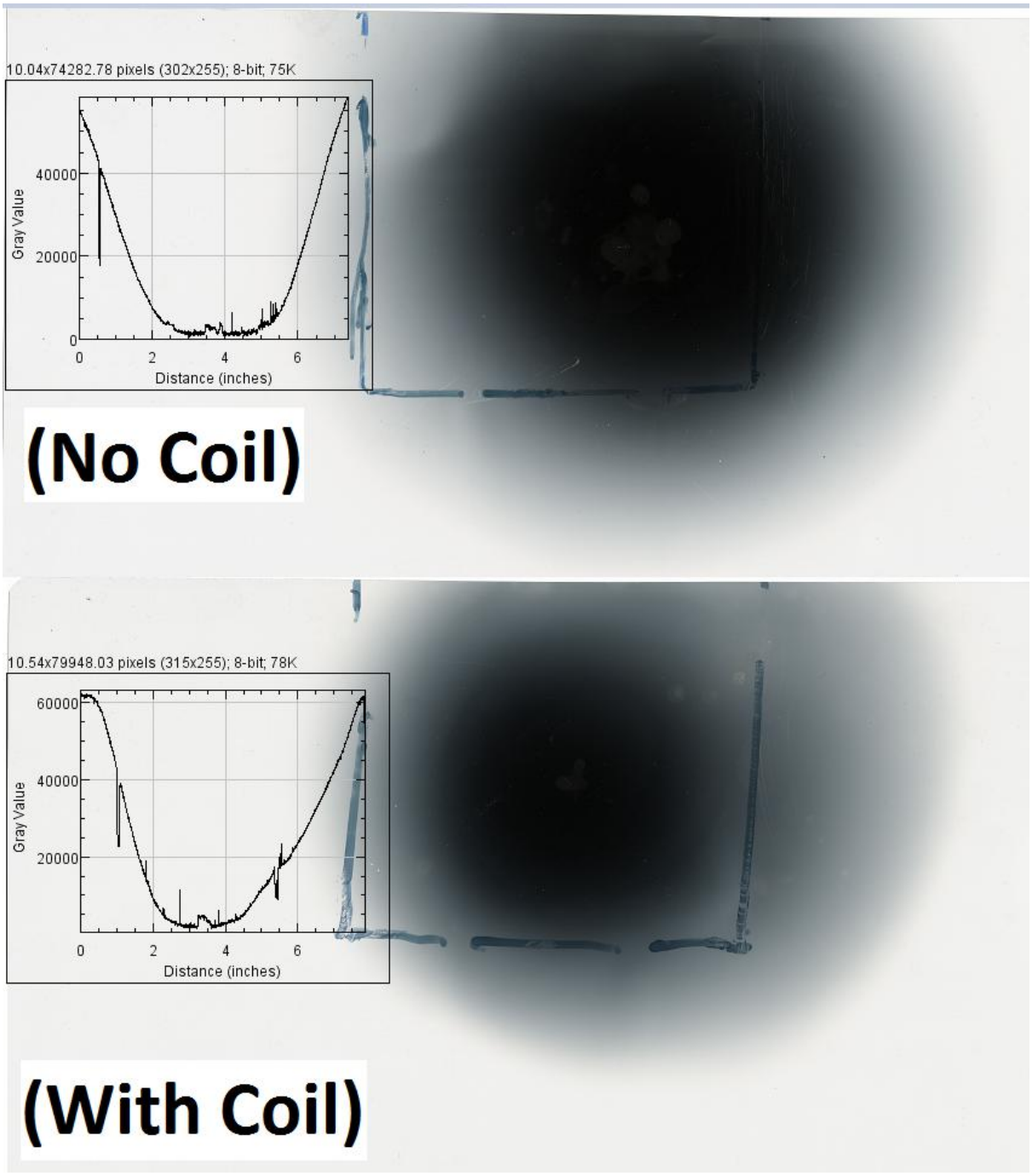

Figure S 5: Deposition patterns used to compute additional calibration factor to account for the plasma plume focussing effect of the magnetic nozzle. The position of the pendulum is shown by the marker pen traces. Inset curves are horizontal transects across the peak deposition zone.

Erosion Rate Measurements

Cathode erosion rates were measured to approximate the system mass flow rate, and thus allow the determination of the Isp and JPE of the various cathode materials tested. The average mass eroded per pulse was determined by weighing the cathode before and after a large number of pulses were fired, and dividing the

difference by the number of pulses after taking into account the cathode cleaning regime [5]. Cathode erosion rates in terms of µg eroded per Coulomb of integrated cathode current were determined by plotting the average mass eroded per pulse against the average integrated cathode current (averaged over the last 128 pulses fired), and applying linear regression trendlines. The slopes of these lines were used to compute the cathode erosion rates for Isp and JPE determination from the thrust measurements undertaken separately, but at similar experimental conditions. The data for Mg and Ti are included here in figure S6, with Data for all materials tested are shown in table S1.

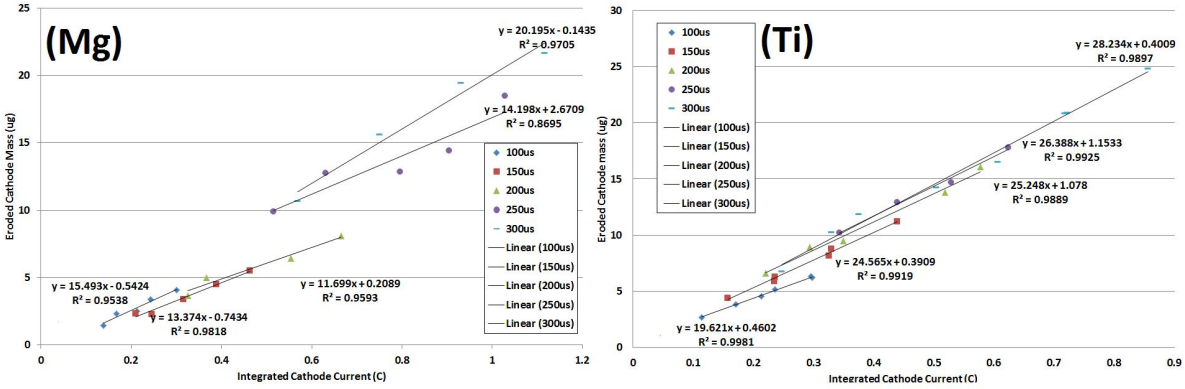

Figure S 6: Mg (left) and Ti (right) cathode erosion rate plots.

Element	100 µs Erosion Rate (µg/C)	150 µs Erosion Rate (µg/C)	200 µs Erosion Rate (µg/C)	250 µs Erosion Rate (µg/C)	300 µs Erosion Rate (µg/C)
Sn	189±32	200±34	377±51	442±29	502±24
Bi	626±71	1090±71	723±41	1260±50	1390±182
Ti	19.6±0.4	24.6±1.1	25.2±1.5	26.4±1.6	28.2±1.2
V	24.5±1.3	25.3±1.8	23.9±1.0	25.1±1.5	23.9±1.2
Cr	24.5±1.9	20.2±3.7	21.9±0.4	22.2±1.2	22.2±0.5
Mo	31.8±2.4	34.7±0.8	34.1±1.2	34.8±0.3	33.4±1.7

Ta	33.6±3.6	50.9±3.0	57.3±1.1	60.0±2.9	55.0±3.2
W	35.2±3.3	43.2±1.9	47.7±0.7	47.7±4.2	48.4±9.9
C	39.6±3.8	31.2±6.1	39.0±1.5	40.8±2.8	31.9±1.2
Mg	15.5±2.0	13.4±1.1	11.7±1.7	14.2±3.2	20.2±2.5
Al	24.4±3.4	25.2±3.1	26.7±2.4	26.0±2.4	24.5±2.7

Table S 1: Erosion rate data for all elements tested

It is clear that the materials with the lowest melting points, being the heavy non-refractory metals tin and bismuth, have by far the highest erosion rates. This is due to the formation of melt pools at the base of the cathode spots due to Ohmic heating of the cathode [32]. These melt pools would then create large quantities of neutral vapour, increasing the erosion rate without contributing significantly to ion production. These high erosion rates lead to the conclusion that Sn and Bi would not be the most efficient materials with which to fuel thrusters. Brown and Shiraishi report the erosion rates of a number of cathodes for 250μs long pulses of 100A [37], and have measured Sn erosion at 295μg/C at these conditions. Our higher erosion rate for Sn is doubtless due to the greater heating developed by the higher arc currents [18].

The similar erosion rates of many of the refractory metals, especially V and Mo, across a wide range of arc durations suggests that they would make dependable fuels for pulsed arc thrusters. The modest erosion rates of these materials also suggest that they would be quite efficient at generating thrust. Our erosion rate results for the refractory metals tend to agree with those of Brown and Shiraishi, as the higher currents have less effect on refractory metal vapour production due to their far lower vapour pressures [30, 37].

The low erosion rate of magnesium is the reason it is the most efficient fuel tested; Mg-fuelled arcs generate appreciable amounts of impulse for the least material eroded from the cathode. The large variation in carbon results indicates that the granular nature of the cathode, combined with the propensity of graphite to trap volatiles, might mean that carbon is a less dependable fuel than many others tested. Brown and Shiraishi did not test carbon cathodes in their work, but our results for Al are in close agreement with theirs; we report a much lower erosion rate for Mg, on the other hand [37]. The difference in Mg erosion rate is probably due to the size of the cathode used; Brown and Shiraishi used 0.25in. cathodes [37] while our work used 25mm cathodes. Work by Daalder has shown that cathode size strongly influences the erosion rate of copper, aluminium and lead targets. Larger cathodes have a lower total erosion rate, while maintaining the same ion generation rate, since larger cathodes are better able to conduct heat away from the heated volume local to the cathode spot [32].